Translationally Invariant Slip-Spring Model for Entangled Polymer Dynamics

Veronica C. Chappa,[1,2,3] David C. Morse,[4] Annette Zippelius,[1] and Marcus Müller[1]

[1]*Institut für Theoretische Physik, Georg-August-Universität, 37077 Göttingen, Germany*

[2]*Departamento de Física, Centro Atómico Constituyentes, Comisión Nacional de Energía Atómica, Av. Gral. Paz 1499, 1650 Pcia. de Buenos Aires, Argentina*

[3]*Consejo Nacional de Investigaciones Científicas y Técnicas, Av. Rivadavia 1917, 1033 Buenos Aires, Argentina*

[4]*Department of Chemical Engineering and Materials Science, University of Minnesota, 421 Washington Ave. S.E., Minneapolis, Minnesota 55455, USA*

(Received 31 May 2012; published 4 October 2012)

The topological effect of noncrossability of long flexible macromolecules is effectively described by a slip-spring model, which represents entanglements by local, pairwise, translationally invariant interactions that do not alter any equilibrium properties. We demonstrate that the model correctly describes many aspects of the dynamical and rheological behavior of entangled polymer liquids, such as segmental mean-square displacements and shear thinning, in a computationally efficient manner. Furthermore, the model can account for the reduction of entanglements under shear.

DOI: 10.1103/PhysRevLett.109.148302 PACS numbers: 83.80.Sg, 61.25.H−, 83.10.Kn, 83.10.Rs

The rheological properties of macromolecular solutions and melts have a significant impact on the polymer processing industry. The fact that two polymer chains cannot cross through each other in the course of their motion does not alter equilibrium properties, but dramatically changes dynamical behavior. To model the rheology of high molecular-weight polymers, Edwards and Doi [1] and de Gennes [2,3] conceived the motion of an entangled chain as reptation along a tube, formed by constraints imposed by the neighboring molecules. While algorithms have been devised to analyze entanglements from the perspective of molecular simulations [4–7], a fully microscopic description of the rheology of polymeric fluids remains a challenge [8–17].

Typically, one enforces noncrossability in coarse-grained bead-spring models by combining a harsh repulsive pair interaction with stiff, nearly inextensible bonds between neighboring beads [4,7,18,19]. This direct approach is invaluable for elucidating the fundamental, molecular nature of entanglements. It is, however, very expensive for simulations of highly entangled polymers. For a typical bead-spring model [18], the simulations of chains with 20 entanglements in a box of size $L = 4R_e$, where R_e denotes the root-mean-squared end-to-end distance, require about 10^{11} molecular dynamics time steps, or 10^2–10^3 processor years with current technology. A systematic study of structure formation in spatially inhomogeneous multicomponent systems, e.g., phase separation in blends or self-assembly of block copolymers, however, requires an alternative approach.

To investigate large-scale properties with a particle-based description, one needs a more coarse-grained model, with fewer beads per chain and softer effective interactions. The softness allows the efficient simulation of systems with realistic values for the invariant degree of polymerization $\bar{\mathcal{N}} \equiv (\rho R_e^3/N)^2$ [20]. This is *inter alia* important for dynamical as well as equilibrium phenomena, because experiments [21,22] and simulations [4–7] have shown that the tube diameter is proportional to $R_e/\sqrt{\bar{\mathcal{N}}}$. However, since such models allow beads to overlap, they do not automatically enforce noncrossability [23]. Padding and Briels proposed to explicitly enforce noncrossability [24,25], but this approach becomes inefficient for dense systems.

Many aspects of the rheology of homogeneous polymer liquids can be accurately reproduced by modeling entanglements between chains by "slip springs," as originally envisaged by Doi and Edwards. Several authors have devised single-chain slip-link models [26–29], in which the chain is constrained at a number of points by slip links, through which the chain can slide. Slip links either have fixed positions, or their positions are constrained by tethers that attach them to fixed points in space. Masubuchi and coworkers [30–32] incorporated entanglement effects into multichain simulations on an extremely coarse-grained level by keeping track only of the positions of slip springs that connect pairs of chains, and treating segments of chains between slip springs as straight segments of the primitive path. To avoid unphysical density variations, the model includes an *ad hoc* repulsion that acts between slip links.

Despite many successes, single-chain models suffer from the following limitations. (i) Since the anchor points are fixed in space, translational invariance is broken and the generalization to complex flows or large deformations is not obvious. (ii) There is no spatial correlation between pairs of slip links that represent constraints imposed on chains by a binary entanglement between them. (iii) The number of slip links is conserved and cannot change in response to rapid flows. In addition to (iii) and the breaking of translation invariance by the Langevin equation of motion, the multichain approach [30,32] (iv) cannot describe

spatial inhomogeneities (e.g., surfaces or interfaces), because the molecular structure between slip links is not resolved and (v) the previous implementation of slip springs alters the equilibrium statistical mechanics in ways that have thus far not been adequately understood.

In this Letter, we propose a multichain slip-spring model that overcomes the above-mentioned limitations of earlier coarse-grained models of entangled liquids, and is suitable for strong flows and inhomogeneous systems. We represent topological constraints by local binary interactions between chains ("slip-springs") that are introduced in a manner that preserves translational and rotational invariance, and leaves all equilibrium properties of the fluid unaltered. We demonstrate that the resulting model captures many dynamical consequences of the topological entanglement in equilibrium and in strong shear flows in a natural and computationally efficient manner.

We first discuss how slip springs can be introduced into a polymer liquid without modifying any equilibrium properties. We consider a system of n polymers, each comprising N beads. Let $\mathbf{r}_i$ denote the position of the ith bead. $\mathcal{H}_0(\{\mathbf{r}\})$ is the potential energy of a bead-spring model without slip springs, comprising bonded interactions between neighboring beads in a chain and nonbonded pair interactions between all beads. In our model, entanglements are represented by slip springs that introduce an additional bonded potential $V_{ss}(r)$ between particular pairs of beads separated by a distance r. The number of slip springs is allowed to fluctuate, and is controlled by an activity $z = \exp(\mu/k_BT)$. Let n_{ij} be the number of slip springs between a particular pair of beads i and j, which is zero for all pairs except those few that are connected by slip springs. The partition function of the system of polymers and slip springs is given by

$$\mathcal{Z} = \int \mathcal{D}[\{\mathbf{r}\}] e^{-\mathcal{H}_0(\{\mathbf{r}\})/k_BT} \prod_{i>j} \sum_{n_{ij}=0}^{\infty} \frac{z^{n_{ij}}}{n_{ij}!} e^{-n_{ij}V_{ss}(|\mathbf{r}_i-\mathbf{r}_j|)/k_BT} \tag{1}$$

where $\mathcal{D}[\{\mathbf{r}\}]$ sums over all conformations [33]. The trace over the slip-spring "occupation numbers" can be explicitly performed, giving

$$\mathcal{Z} = \int \mathcal{D}[\{\mathbf{r}\}] e^{-\mathcal{H}_0(\{\mathbf{r}\})/k_BT} \exp\left(\sum_{i<j} z e^{-V_{ss}(|\mathbf{r}_i-\mathbf{r}_j|)/k_BT}\right) \tag{2}$$

The effect of introducing slip springs on equilibrium properties is seen to be equivalent to the addition of an attractive potential

$$\Delta\Phi(r) = -zk_BTe^{-V_{ss}(r)/k_BT} \tag{3}$$

between all pairs that can be connected by slip springs. Thus, we can exactly compensate the effect of slip springs on equilibrium properties by adding a repulsive potential $-\Delta\Phi(r)$ to the pair potential of the original Hamiltonian $\mathcal{H}_0$. The total potential energy of the resulting model is given by a sum of the Hamiltonian $\mathcal{H}_0$ of the unentangled liquid, a slip-spring bonded potential that acts only between beads that are connected by slip springs, and an additional compensating potential $-\Delta\Phi(r)$ that acts between all monomers that are allowed to be connected with slip springs.

In the present work, neighboring beads along a chain are bonded together via a harmonic potential $V_b(r) = \frac{1}{2}k_br^2$, where r is the distance between particles. In the absence of slip springs, nonbonded pairs interact by a bare pair potential of the form $V_{nb}(r) = \frac{\epsilon}{2}(1 - r/\sigma)^2$ for $r < \sigma$ [34]. The slip-spring potential is modeled by a finitely extensible nonlinear elastic potential $V_{ss}(r) = -\frac{1}{2}k_{ss}r_{ss}^2 \ln[1 - (r/r_{ss})^2]$, which diverges as $r \to r_{ss}$ [35]. We choose a finite-range potential for the slip springs because the range of the compensating potential $-\Delta\Phi(r)$ is the same as the range of allowed values of the slip-spring bond length. We choose r_{ss} to be comparable to the range σ of the bare nonbonded interaction to avoid any large increase in the number of nonbonded neighbor interactions. In the present work, we use $k_b = 12k_BT/\sigma^2$, $\epsilon = 24k_BT$, $r_{ss} = 1.2\sigma$, $k_{ss}r_{ss}^2/2 = 17.28k_BT$, and a bead density $\rho\sigma^3 = 2$.

The conformation of polymers and slip springs are updated by a hybrid Monte Carlo (MC) scheme. At each time step, we choose with fixed probabilities between a "move" that updates the segment positions by a short molecular dynamics simulation [36] with a dissipative particle dynamics (DPD) thermostat [37,38] and one of several MC moves illustrated in Fig. 1 that can move, create, or destroy slip springs. We use a DPD friction coefficient $\gamma = 0.5k_BT\tau_{MD}/\sigma^2$ and an integration time step of $\Delta t = 0.01\tau_{MD}$, where $\tau_{MD} = \sqrt{m\sigma^2/k_BT}$ and m denotes the bead mass. Each such short DPD move is chosen with a probability 0.5, and propagates the conformations by τ_{MD}, corresponding to a bead displacement of order of the bond length. This integration scheme conserves momentum, resulting in hydrodynamic behavior on long time and length scales. Otherwise, we update the slip-spring configuration with one of the MC moves. The

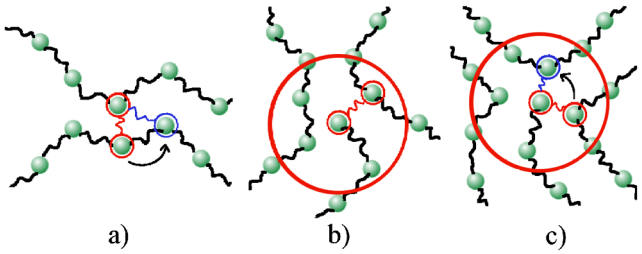

FIG. 1 (color online). Monte Carlo updates of slip-spring conformations: (a) Shuffling of a slip spring along the backbone of a chain molecule (reptation), (b) grand canonically creating or deleting a slip spring at a chain end, and (c) transferring one end of a slip spring from one chain to another bead (constraint release and re-entanglement).

"shuffle" move [Fig. 1(a)] transfers one end of a slip spring from one segment to the neighboring one along the same chain, and is accepted with a Metropolis acceptance probability. This move allows reptation of a chain through a slip spring. The "create-destroy" move shown in Fig. 1(b) instead allows a slip spring to be deleted or a new slip spring to be created at a chain end, and is necessary to maintain a fixed activity for slip springs. To add a slip spring at the chain end, we select one slip-spring partner according to its Boltzmann factor e^{-V_{ss}/k_BT} among the n_0 possibilities with slip-spring lengths Δr_i, and accept this move with probability $\min(1, \frac{nNz}{n_{ss}+1} \sum_{i=1}^{n_o} e^{-V_{ss}(\Delta r_i)/k_BT})$, where nN is the total number of segments and n_{ss} the number of slip springs before the move. A related acceptance condition is applied to the reverse move, slip-spring deletion, in order to fulfill detailed balance. The transfer move shown in Fig. 1(c) can be applied when one end of a slip spring is at the chain end and transfers the other end to another bead that may belong to another chain. To this end, one of all possible slip-spring partners within the range of V_{ss} is chosen with a probability proportional to the Boltzmann factor e^{-V_{ss}/k_BT}. This move mimics the destruction of an entanglement and the rapid re-creation of a new entanglement. To rapidly generate equilibrated starting configurations, we can also use a move (not shown) that can create or destroy slip springs between any two segments, anywhere along a chain. In simulations that are used to study dynamical behavior, however, we allow slip springs to be created and destroyed only at the chain ends.

We control the slip-spring activity, z, rather than their number. The inset of Fig. 2 presents the linear dependence of the average concentration of slip springs on their activity (see Supplemental Material [39]). As expected, the slip-spring concentration is almost independent of chain length N. Figure 2 demonstrates the importance of the compensating potential in a system with a low bead density, $\rho\sigma^3 = 0.22$. In the absence of the compensating potential, upon increasing the slip-spring activity z, we observe a chain collapse. With the compensating potential, the chain size remains independent of z. The effect of the uncompensated effective attraction induced by slip springs is less dramatic in denser liquids, but is always present, and can be qualitatively important in some situations, e.g., at liquid-vapor coexistence, where a small additional attraction may cause cavitation.

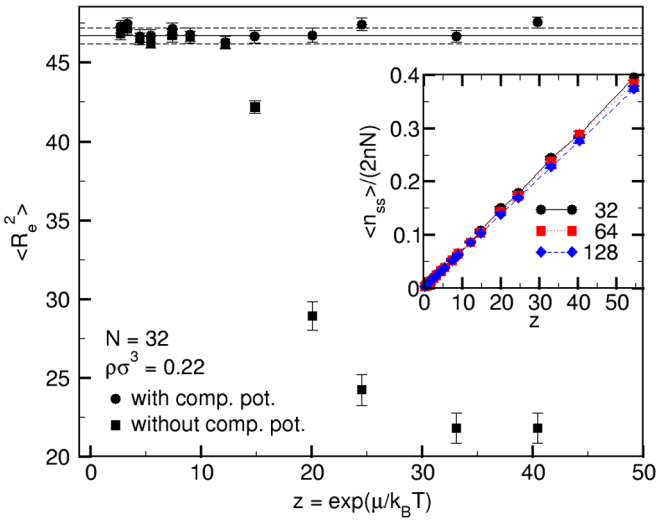

FIG. 2 (color online). Chain dimensions R_e as a function of the activity of slip springs at density $\tilde{\mathcal{N}} = 4$, without and with compensating potential $-\Delta\Phi$. Inset: Average number $\langle n_{ss}\rangle/(2nN)$ of slip springs per monomer as a function of the slip-spring activity z.

While the combination of slip springs and compensating potential does not affect chain conformations, it has pronounced consequences for the dynamics. In Fig. 3, we present the mean-square displacement $g_1(t)$ for all segments with and without slip springs for $N = 128$. The activity of slip springs is adjusted to $z = 35.87$, yielding on average 32 slip springs per chain. Without slip springs, the single-chain dynamics is very close to Rouse dynamics [40], for which $g_1(t) \propto t^{1/2}$ at intermediate times. With slip springs, the segment motion is significantly slowed down, and the different power laws predicted by the tube theory emerge naturally. Note the appearance of a wide regime in which $g_1(t) \propto t^{1/4}$, as expected for highly entangled chains at times between the entanglement and Rouse times.

The tube model is an idealized theory of the dynamics of entangled polymers. It has two phenomenological

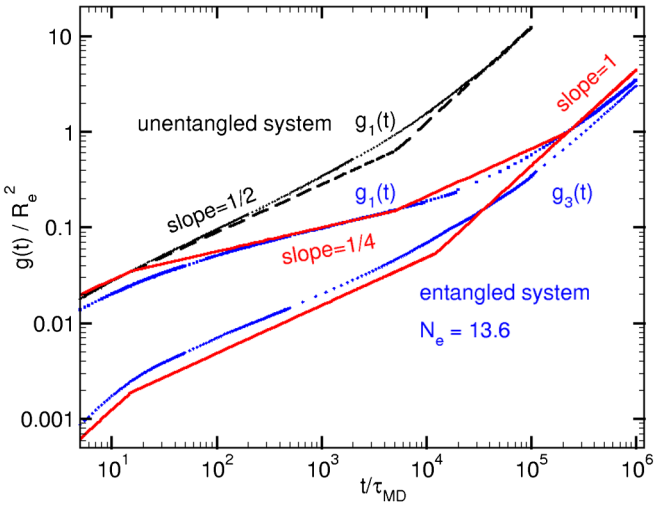

FIG. 3 (color online). Mean-square displacement $g_1(t)$ of all segments and of the molecule's center of mass g_3, with and without slip springs for $N = 128$. The activity of slip springs is $z = 35.87$, resulting in an average distance between the slip springs of four segments; $\langle R_e^2\rangle = 114 \pm 1\sigma^2$. The simulation cell size is $L = 20\sigma$. The lines show the predictions of the tube model, where N_e is extracted from the behavior $g_1 \propto t^{1/4}$ of the entangled system and the measured self-diffusion coefficient D of the unentangled system.

parameters: A segment friction coefficient ζ and an entanglement length N_e. We can infer values for ζ and N_e for our more microscopic slip-spring model by comparing simulation results for $g_1(t)$ to tube model predictions. Since the segment displacements of our models with and without slip springs coincide at short times, the friction coefficients for these two models are approximately equal. We extract a value for ζ from the long-time diffusion coefficient $D = \lim_{t\to\infty} g_1(t)/6t$ of the unentangled system by using the Rouse model, setting $D = k_B T/\zeta N$. To extract a value for N_e, we then fit the behavior of $g_1(t)$ for the entangled system (with slip springs) in the intermediate $t^{1/4}$ regime [41] (cf., Supplemental Material [39]). This leads to the estimate $N_e = 13.6$. We determined N_e by fitting behavior in this $t^{1/4}$ regime, rather than from the long-time diffusion coefficient, because we expect the dynamical behavior at late time to be significantly affected by contour length fluctuation effects that are captured by our slip-spring model, but not by the idealized tube model. Our estimate implies that, for our model, one entanglement is represented by roughly three slip springs.

We have used the reverse nonequilibrium molecular dynamics (RNEMD) method [42] to simulate a steady shear flow. In this scheme, we divide the simulation cell into two halves, separated by narrow bands in which controllable opposing forces are applied by exchanging momenta between pairs of particles in these two bands. This creates a sawtooth velocity profile that contains two wide regions with opposing, nearly homogeneous velocity gradients. The viscosity, $\eta(\dot\gamma) = \sigma_{xz}/\dot\gamma$, is calculated from the velocity gradient $\dot\gamma = \partial\langle v_x(z)\rangle/\partial z$ in the middle of these regions.

Figure 4 presents the viscosity, $\eta = \sigma_{xz}/\dot\gamma$, as a function of shear rate. We define the Weissenberg number by $\mathrm{Wi} \equiv \dot\gamma R_e^2/D$. For a small Wi, we observe a Newtonian plateau characterized by a viscosity that increases with chain length, N. Experiments on entangled polymer melts yield a Newtonian viscosity $\eta_0 = \lim_{\dot\gamma\to 0}\eta(\dot\gamma)$ that varies with N as $\eta_0(N) \propto N^x$, where $x = 3.4$ [1]. The ratio of the Newtonian viscosities for the two chain lengths considered here, $N = 32$ and 64, gives $x = 3.55$, which is very similar to that observed in experiments. For high shear rates, we observe shear thinning, and η becomes independent of N. The viscosity obeys a power law, $\eta \sim \mathrm{Wi}^{-\alpha}$, with $\alpha \simeq 0.64$, in reasonable agreement with experiments [43]. In this nonlinear regime, we also observe a pronounced deformation of molecular conformations.

Since we perform the simulations in an ensemble with a fluctuating number of slip springs, at a constant activity z, the average number of slip springs per chain can change with shear rate. Interestingly, we observe a modest decrease in the number of slip springs with increasing shear rate. This is a natural result of flow-induced retraction of the chain ends in the tube model [1], which tends to sweep individual entanglements towards the end of the chains, where they can be destroyed. We have confirmed that this

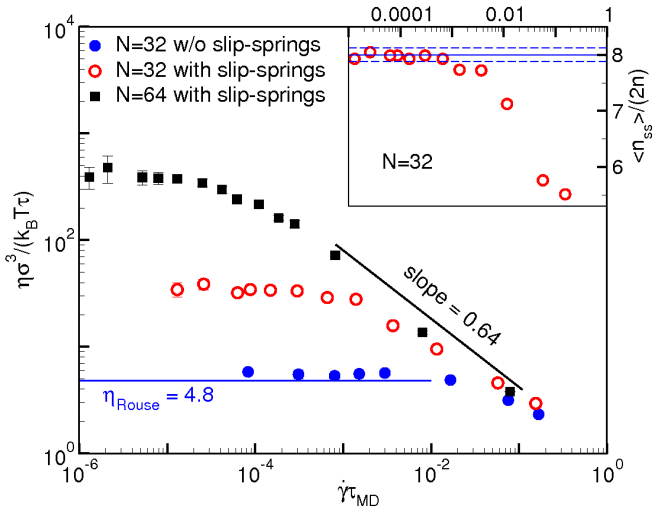

FIG. 4 (color online). Main panel: Shear viscosity η as a function of shear rate $\dot\gamma$ for the system with and without slip springs. The slip-spring activity results in approximately four monomers between slip springs in equilibrium. Inset: Decrease of the number of entanglements per chain with shear rate $\dot\gamma$ for $N = 32$.

phenomenon is independent of the frequency of MC moves that attempt to create and destroy slip springs at the chains ends, as long as this frequency exceeds a minimum value much lower than that used in our simulations. We believe that the phenomenon is inherent in any model that allows entanglements to be created and destroyed only at chain ends, that allows for flow-induced retraction, and that does not artificially constrain the total number of slip springs.

In summary, we have presented the effect of entanglements in polymer liquids without explicitly enforcing noncrossability by binary, local slip springs. Our model retains the equilibrium properties of the original model without slip springs. Similar to Likhtman's slip-link model, our model describes the effect of entanglements on the single-chain dynamics and viscosity in equilibrium. The model automatically incorporates contour length fluctuations and constraint release. Because it preserves translation invariance, our model additionally can be applied to problems involving flow and strong deformations. We demonstrate that the model exhibits realistic shear thinning, deformation of conformations, and a decrease of the number of entanglements at high shear rates. While we have only considered bulk homopolymer melts, our model can be generalized to thin films or multicomponent polymer liquids, e.g., homopolymer blends or diblock copolymers materials [44], branched or star molecular architectures, and entangled networks. The model is also well suited to study time-dependent flows, such as step strain and start-up of continuous shear, which is controversial in the literature.

We have benefited from stimulating discussions with A. E. Lihtkman, A. Ramírez-Hernández, and

J. J. de Pablo. DCM thanks the SFB 602 and the Göttingen Academy of Science for hospitality during his sabbatical stay in Göttingen. Financial support by the SFB 602 and computing time at the HLRN Hannover and Berlin and the JSC Jülich, Germany, are gratefully acknowledged.

[1] M. Doi and S. F. Edwards, *The Theory of Polymer Dynamics* (Clarendon Press, Oxford, 1986).
[2] P. G. de Gennes, J. Chem. Phys. **55**, 572 (1971).
[3] P. G. de Gennes, Macromolecules **9**, 587 (1976).
[4] R. Everaers, S. K. Sukumaran, G. S. Grest, C. Svaneborg, A. Sivasubramanian, and K. Kremer, Science **303**, 823 (2004).
[5] M. Kröger, Comput. Phys. Commun. **168**, 209 (2005).
[6] C. Tzoumanekas and D. N. Theodorou, Macromolecules **39**, 4592 (2006).
[7] N. Uchidaa, G. Grest, and R. Everaers, J. Chem. Phys. **128**, 044902 (2008).
[8] C. Tzoumanekas and D. N. Theodorou, Curr. Opin. Solid State Mater. Sci. **10**, 61 (2006).
[9] M. Guenza, J. Phys. Condens. Matter **20**, 033101 (2008).
[10] A. E. Likhtman, J. Non-Newtonian Fluid Mech. **157**, 158 (2009).
[11] J. P. Wittmer, H. Meyer, A. Johner, T. Kreer, and J. Baschnagel, Phys. Rev. Lett. **105**, 037802 (2010).
[12] J.-X. Hou, C. Svaneborg, R. Everaers, and G. S. Grest, Phys. Rev. Lett. **105**, 068301 (2010).
[13] J. Cao and A. E. Likhtman, Phys. Rev. Lett. **104**, 207801 (2010).
[14] D. M. Sussman and K. S. Schweizer, Phys. Rev. Lett. **107**, 078102 (2011).
[15] D. M. Sussman and K. S. Schweizer, J. Chem. Phys. **135**, 131104 (2011).
[16] J. Farago, H. Meyer, and A. N. Semenov, Phys. Rev. Lett. **107**, 178301 (2011).
[17] J. Cao and A. E. Likhtman, Phys. Rev. Lett. **108**, 028302 (2012).
[18] G. S. Grest and K. Kremer, Phys. Rev. A **33**, 3628 (1986).
[19] K. Kremer and G. S. Grest, J. Chem. Phys. **92**, 5057 (1990).
[20] M. Müller, J. Stat. Phys. **145**, 967 (2011).
[21] L. J. Fetters, D. J. Lohse, S. T. Milner, and W. W. Graessley, Macromolecules **32**, 6847 (1999).
[22] L. J. Fetters, D. J. Lohse, and W. W. Graessley, J. Polym. Sci., Part B: Polym. Phys. **37**, 1023 (1999).
[23] M. Müller and K. C. Daoulas, J. Chem. Phys. **129**, 164906 (2008).
[24] J. T. Padding and W. J. Briels, J. Chem. Phys. **115**, 2846 (2001).
[25] J. T. Padding and W. J. Briels, J. Chem. Phys. **117**, 925 (2002).
[26] A. E. Likhtman, Macromolecules **38**, 6128 (2005).
[27] J. Ramirez, S. K. Sukumaran, and A. E. Likhtman, J. Chem. Phys. **126**, 244904 (2007).
[28] D. M. Nair and J. D. Schieber, Macromolecules **39**, 3386 (2006).
[29] J. D. Schieber, D. M. Nair, and T. Kitkrailard, J. Rheol. **51**, 1111 (2007).
[30] Y. Masubuchi, J. I. Takimoto, K. Koyama, G. Ianniruberto, G. Marrucci, and F. Greco, J. Chem. Phys. **115**, 4387 (2001).
[31] J. Oberdisse, G. Ianniruberto, F. Greco, and G. Marrucci, Rheol. Acta **46**, 95 (2006).
[32] Y. Masubuchi, T. Uneyama, H. Wanatabe, G. Ianniruberto, F. Greco, and G. Marrucci, J. Chem. Phys. **132**, 134902 (2010).
[33] The above analysis allows for several variations, distinguished by whether or not we allow a single pair of beads to be connected by more than one slip spring, and by different choices of which pairs we allow to be connected by slip springs. We allow slip links to exist between all segments except those that are already connected by covalent bonds, and allow an arbitrary number of slip springs to form between any pair segments (Bose statistics), as implied by the sum of $n_{ij} = 0, \ldots, \infty$. Alternatively, we could have implemented Fermi statistics, with $n_{ij} \leq 1$. Since $\langle n_{ij} \rangle \sim \sigma^3/V \ll 1$ (see Supplemental Material at http://link.aps.org/supplemental/10.1103/PhysRevLett.109.148302 [39]) we would expect nearly identical results.
[34] R. D. Groot and P. B. Warren, J. Chem. Phys. **107**, 4423 (1997).
[35] Note that our slip-spring potential is anharmonic; alternative forms could be used (see [15]).
[36] P. Nikunen, M. Karttunen, and I. Vattulainen, Comput. Phys. Commun. **153**, 407 (2003).
[37] P. J. Hoogerbrugge and J. M. V. A. Koelman, Europhys. Lett. **19**, 155 (1992).
[38] P. Warren and P. Espanol, Europhys. Lett. **30**, 191196 (1995).
[39] See Supplemental Material at http://link.aps.org/supplemental/10.1103/PhysRevLett.109.148302 for the equation of state for the slip springs and the asymptotic forms of the mean-square displacements in the Rouse and tube models.
[40] P. E. Rouse, J. Chem. Phys. **21**, 1272 (1953).
[41] A. E. Likhtman and T. C. B. M. Leish, Macromolecules **35**, 6332 (2002).
[42] F. Müller-Plathe, Phys. Rev. E **59**, 4894 (1999).
[43] R. Stratton, J. Colloid Interface Sci. **22**, 517 (1966).
[44] A. Ramírez-Hernández *et al.*, (to be published).